Inorganic Chemistry

Article

pubs.acs.org/IC

Synthesis, Structural Characterization, and Ab Initio Study of $Cu_{5+\delta}In_{2+x}Sb_{2-x}$: A New B8-Related Structure Type

Carola J. Müller,*[,†] Sven Lidin,[†] Susana Ramos de Debiaggi,[‡,§] Crispulo E. Deluque Toro,[‡] and Armando Fernández Guillermet[§,⊥]

[†]Polymer and Materials Chemistry, Lund University, Lund, Sweden

[‡]Departamento de Física, Facultad de Ingeniería, Universidad Nacional del Comahue, Neuquén Province, Argentina

[§]CONICET, Santa Fe, Argentina

[⊥]Unidad de Actividad de Física, Física de Metales, Centro Atómico Bariloche, S. C. de Bariloche, Argentina

Supporting Information

ABSTRACT: A new ternary orthorhombic compound with the formula $Cu_{5+\delta}In_{2+x}Sb_{2-x}$, crystallizing in the space group $Cmc2_1$ with 36 atoms per unit cell [a = 10.1813(4) Å, b = 8.4562(4) Å, c = 7.3774(2) Å, Z = 4], has been synthesized by conventional high-temperature methods. The structure is based on the B8 archetype (NiAs/Ni_2In) and features In/Sb ordering as well as ordering of interstitial copper. Details of the experimental study and the structural parameters of this compound are reported in the first part of the work. In the second part, *ab initio* calculations based on the density functional theory and the projector augmented-wave method are used to characterize the structural, thermodynamic, and phase-stability properties of the new ternary phase. The present calculations include the lattice parameters, molar volume, bulk modulus and its pressure derivative, the energy of formation from the elements, and the electronic density of states. Moreover, the present *ab initio* method is used to investigate the thermodynamic properties of the anti-structure $Cu_5Sb_2In_2$ compound obtained by exchanging the In and Sb Wyckoff symmetric positions.

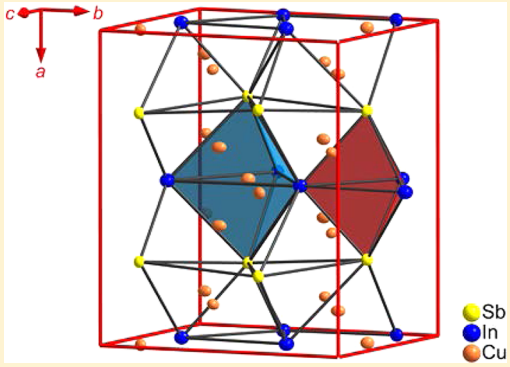

1. INTRODUCTION

The study of the stable phases in the Cu−In−Sb system is of interest in connection with the contact metallurgy of InSb, a narrow gap semiconductor compound with a very high electron mobility, that is widely used in a variety of electronic devices. It is also of relevance for the design of lead-free soldering alloys.[1] In spite of the practical relevance of the Cu−In−Sb alloys, the phase diagram and the properties of the compounds occurring in this system have not yet been accurately determined. In fact, the most recent attempts to establish the ternary phase diagram involve extrapolations based on thermodynamic models.[2,3] While this may yield useful insights into pseudobinary system behavior, it will not predict the occurrence and constitution of true ternary phases. The purpose of the present paper is to report a combined experimental and theoretical study of a ternary Cu−In−Sb compound that was detected in the framework of a study of the η phase, a common equilibrium phase of both the Cu−In[4,5] and Cu−Sn binary systems.[6−8]

The B8 phase field (NiAs/Ni_2In structure types) in the binary system Cu−In is complex and comprises at least four well-defined regions (Figure 1). The indium-rich side of the phase field contains the line compounds $Cu_{11}In_9$ and $Cu_{10}In_7$, while the (internal) η-phase field is centered around the composition Cu_2In. The copper-rich side is dominated by the phase Cu_7In_3, which has a rather broad existence interval ($Cu_{7.2-\delta}In_{2.8+\delta}$; $0 \le \delta \le 0.4$). The structure of the η-phase field in the Cu−In binary system has not yet been fully resolved, although it is accepted that it involves at least one high-temperature (HT) phase (η') and at least one at low temperature (LT, η).[9]

The η'/η transition temperature depends upon the composition.[10] The HT structure is of the type NiAs/Ni_2In with random partial occupation of the Cu sites with 2d symmetry, whereas the LT phase presents modulated superstructures based on the B8−NiAs/Ni_2In prototype, with an ordered distribution of defects at sites (2d).[11]

On the other hand, there are no B8-type binary Cu−Sb phases. The copper-rich side of the phase diagram consists of $Cu_{11}Sb_3$,[12] $Cu_{10}Sb_3$,[13] and HT1-Cu_3Sb,[14] which are colored hexagonal close packings. While HT2-Cu_3Sb[15] adopts the BiF_3 structure type, Cu_2Sb crystallizes in a structure featuring puckered slabs of colored cubic close packing.[16] Full solid solubility in the ternary system is impossible.

In this paper, we report on the synthesis and characterization of a new ternary phase in the Cu−In−Sb system. Subsequent to

Received: June 2, 2012
Published: October 2, 2012

   dx.doi.org/10.1021/ic3011794 | *Inorg. Chem.* 2012, 51, 10787−10792

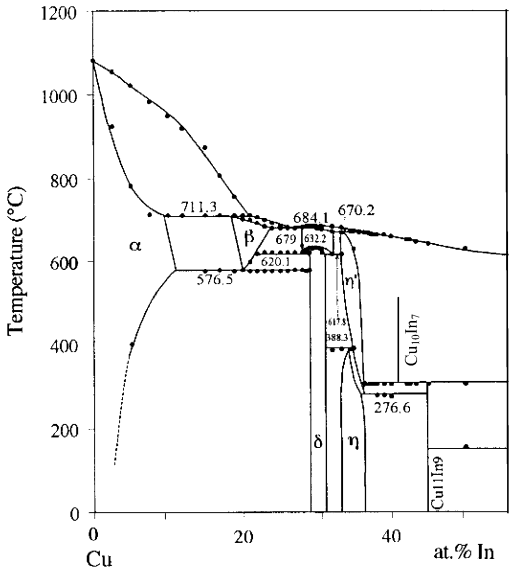

Figure 1. Copper-rich side of the Cu−In phase diagram. Adapted from Bahari et al.[5]

the synthesis, energy-dispersive X-ray spectroscopy (EDXS) was used to determine the composition of the new compound and the structure was solved and refined by X-ray diffraction analysis. In the second, theoretical part of the paper, *ab initio* calculations based on the density functional theory (DFT) and the projector augmented-wave method[17] (PAW), implemented in the VASP code,[18] were used to establish the theoretical electronic, cohesive, and thermodynamic properties of an idealization of the new compound $Cu_5In_2Sb_2$. For comparison, the $Cu_5Sb_2In_2$ anti-site phase, resulting from exchange of the indium and antimony Wyckoff positions, was analyzed as well.

2. EXPERIMENTAL SECTION

2.1. Synthesis. Elemental copper (ABCR, Karlsruhe, shots, 99.99%), indium (Chempur, ingots, 99.9999%), and antimony (Chempur, shots, 99.999%) were reacted in a molar ratio of 6:3:2 (Cu:In:Sb) in an argon-purged, evacuated silica ampule at 900(5) °C in a muffle furnace for 3 days. After furnace cooling, the sample was placed in an aluminum block and annealed at 300(5) °C in a muffle furnace for 30 days.

2.2. Characterization. Powder X-ray diffraction experiments were performed in transmission mode on a Stoe Stadi MP (vertical set-up), equipped with a curved germanium monochromator (Johan geometry) and a MYTHEN detector, using Cu Kα_1 radiation. The zero point of the diffractometer was aligned against silicon. Diffractometer control and data analysis were performed using *WinXPow*.[19]

Single crystals were isolated from the resulting ingot after crushing. A triangular fragment with clean cleavage surfaces and metallic luster was chosen for the X-ray experiment and mounted on a silica fiber using a standard two-component adhesive. The data collection was performed on an XCalibur 3 single-crystal diffractometer at ambient conditions using monochromatized Mo Kα radiation (0.71073 Å) and a Sapphire III detector. The program suite *CrysAlisPro*[20] was used for data reduction and integration, while charge flipping,[21,22] as implemented in *Superflip*,[23] was applied for structure solution and *Jana2006*[24] for the following structure refinement.

Pieces of 20−25 mm^2 were embedded in epoxy, ground with SiC paper, and polished with a diamond suspension as the final step for the scanning electron microscopy experiments. Those were performed on a JEOL 3000 with a secondary electron (SEI) detector and a backscatter detector for EDXS measurements. *AZtec*[25] was employed for data analysis of the spectra.

3. THEORETICAL SECTION

The total energy calculations were performed using the projector augmented-plane-wave method and the *VASP* code. We adopt the conjugate gradient approximation due to Perdew and Wang (GGA-PW91).[26] The cutoff kinetic energy for the plane-wave expansions was 330 eV. For the PAWs, we considered 11 valence electrons for Cu ($3d^{10}4s^1$), 3 for In ($5s^25p^1$), and 5 for Sb ($5s^25p^3$). The *k*-point mesh was verified for the energy to be converged within 1 meV/atom. Specifically for $Cu_5In_2Sb_2$, we considered a mesh of 9 × 11 × 13, leading to 210 *k* points in the irreducible Brillouin zone. The self-consistent criterion for the energy was 0.1 meV. Finally, the structure was optimized with respect to lattice parameters and internal degrees of freedom. From the calculated total energies of $Cu_5In_2Sb_2$, the anti-site structure $Cu_5Sb_2In_2$, and the elements copper, indium, and antimony, we obtained the energy of formation (ΔE_f) of the compounds.

4. RESULTS AND DISCUSSION

4.1. Experimental Composition and Structure of the New Phase. The sample contains three compositionally distinct compounds: the target compound and the well-known phases InSb and Cu_7In_3. The EDX composition of InSb is $In_{51}Sb_{49}$ and that of Cu_7In_3 is $Cu_{72}In_{28}$, indicating a reliability of the compositional analysis within 1 or 2%. When this is applied to the title phase, the composition of $Cu_{58}In_{24}Sb_{18}$ is well described by $Cu_{5+\delta}In_{2+x}Sb_{2-x}$ ($\delta \approx 0.33$; $x \approx 0.29$) (Figure 2).

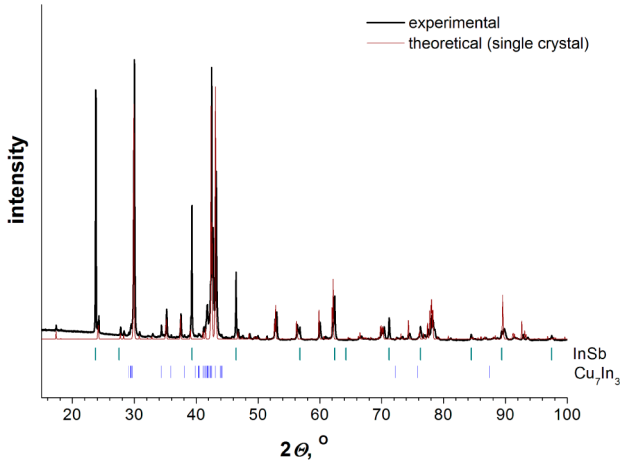

Figure 2. Powder X-ray diffraction pattern of $Cu_{5+\delta}In_{2+x}Sb_{2-x}$. The phase Cu_7In_3 is present as a minor component, and its theoretical pattern overlaps with some strong reflections (I_{rel} > 10%).

4.2. Powder X-ray Diffraction. Three compounds could be identified in the powder X-ray diffraction pattern of the sample: InSb, Cu_7In_3, and the title compound. The latter has been indexed by a comparison to a calculated theoretical powder pattern from the single-crystal data (see section 4.3). The lattice parameters have been refined to a = 10.1813(4) Å, b = 8.4562(4) Å, and c = 7.3774(2) Å. No extra reflections were observed.

4.3. Single-Crystal X-ray Diffraction. A preliminary inspection of the diffraction pattern revealed a set of strong substructure reflections indicating a basic NiAs/Ni_2In-type structure and additionally satellite reflections quadrupling the a and b axes and doubling c (Figure 3 and Table 1). A closer

dx.doi.org/10.1021/ic3011794 | Inorg. Chem. 2012, 51, 10787−10792

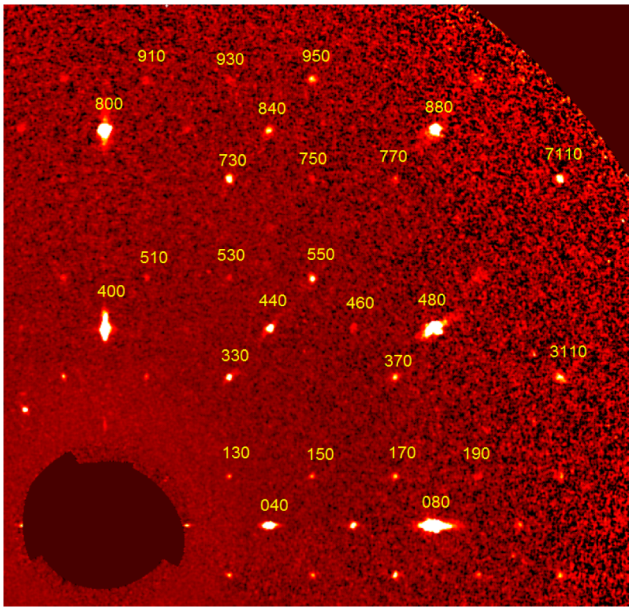

Figure 3. Reconstructed reciprocal lattice layer *hk*0 (in hexagonal setting, *c** is vertical and *a** is horizontal). Note the presence of weak satellites doubling *c* and quadrupling *a*. Reflections with odd *l* indices in the fundamental B8-type structure are constitutionally weak.

Table 1. Data Collection and Refinement Details for $Cu_{5+\delta}In_{2+x}Sb_{2-x}$

chemical formula from refinement; from EDXS	$Cu_{5.33}In_2Sb_2$; $Cu_{5.33}In_{2.29}Sb_{1.71}$
space group; *Z*	$Cmc2_1$ (No. 36)
lattice parameters from powder, Å	a = 10.1813(4), b = 8.4562(4), c = 7.3774(2) (from powder X-ray diffraction)
volume, Å^3	635.16(3)
temperature, K	295(1)
density (calcd), g/cm^3	8.3019
λ, Å	0.71073
reflections/parameter	1176/54
μ, mm^2	32.3
R_{obs}; wR_{obs}; R_{all}; wR_{all}	0.060; 0.058; 0.090; 0.063
twin law	(1 0 0, 0 $-^1/_2$ $-^3/_4$, 0 1 $-^1/_2$) (1 0 0, 0 $-^1/_2$ $^3/_4$, 0 −1 $-^1/_2$)
twin fractions	0.11(3); 0.14(3)

inspection of the intensity distribution of the satellite reflections clearly indicated a lowering of the symmetry from hexagonal to orthorhombic. Consequently, a twinned, orthorhombic symmetry, compatible with the extinction conditions and the allowed group−subgroup relations, needed to be identified.

Moreover, the *C*-centering, generated by the transformation from hexagonal to orthorhombic symmetry, is violated by superstructure reflections. A new centering is introduced in the augmented 2 × 1 × 2 orthorhombic supercell, resulting in a pattern that is characteristic for the space group *Bbmm*. However, this group is disallowed by the group−subgroup relations since the doubling of the hexagonal *c* axis will violate the *c* glide. The maximal space group is therefore uniquely determined to $Bb2_1m$ ($Cmc2_1$ in the conventional setting). The corresponding group−subgroup relations are shown in Scheme 1, together with the accompanying orbit splitting.

It is notable that the In position (2*c*) and the partially occupied Cu position (2*d*) are both split into three independent positions (8*b*, 4*a*, and 4*a*) with the relative multiplicities 2:1:1. This allows perfect In/Sb order and provides a site that corresponds to a $^1/_4$ occupancy of the second Cu position. The Wyckoff position that is fully occupied by copper in the basic model splits into two equivalent orbits (Cu1 on 8*b* and Cu2 on 8*b*).

A starting model was generated using *Superflip*.[23] This refined satisfactorily to a fully ordered structure, $Cu_5In_2Sb_2$ in the space group $Cmc2_1$ (Figure 4).

In this ordered model, antimony and indium are arranged in such a way as to avoid homoatomic contacts. Together they form a hexagonal close packing *ABAB*, where alternating layers are composed exclusively of antimony (*A*) or indium (*B*). This creates only one kind of octahedral interstices (all filled by copper) but two different kinds of trigonal-bipyramidal interstices: one with apical antimony and equatorial indium and another in which these roles are reversed. Only half of the former are filled by copper, while the latter are empty. From structural images, it is obvious that the apical antimony relaxes substantially away from the occupied sites and toward the vacant sites. As an outcome, the inter-apex distance in empty trigonal-bipyramidal interstices is 4.8 Å, while the corresponding value for filled interstices is 5.4 Å.

Returning to the results of the EDX analysis, it is perspicuous that the fully ordered model is not completely correct. Clearly, the position assigned to contain only antimony must also contain a small amount of indium. Given the small difference in the scattering power between these two elements, it is understandably meaningless to try to refine this. Further, the slight overoccupancy of copper must reside somewhere, and the most obvious place to look is in the empty 4*a* and 8*b* positions. There is no support for any occupancy in the 8*b* position, but a copper atom in the 4*a* position with the ideal coordinates ($^1/_2$, $^7/_8$, $^1/_{12}$) refines to an occupancy of 0.175 and yields a total copper content close to 1.3 times that of the sum of indium and antimony. The trigonal bipyramids with indium apexes are completely unoccupied, while for those with apexes that are predominantly antimony, every second interstice is fully occupied while the remaining are randomly occupied to about $^1/_6$.

The data pertinent to the structural work may be found in the Supporting Information.

4.4. Ab Initio Calculated Properties. The ordering of indium and antimony in $Cu_5In_2Sb_2$ is reasonable from a chemical point of view, but the evidence is not so strong given the similarity of their scattering factors for X-rays. It is therefore valuable to compare the relative stability of this compound with the In/Sb site-inverted compound: $Cu_5Sb_2In_2$. In Table 2, we present the *ab initio* results for the equilibrium volume (V_0), lattice parameters, bulk modulus (B_0) and its pressure derivative (B_0'), and energy of formation (ΔE_f) obtained in the generalized gradient approximation (GGA) for the elements copper, indium and antimony in their equilibrium structures, for $Cu_5In_2Sb_2$, and for the $Cu_5Sb_2In_2$ anti-structure compound, resulting from exchange of the indium and antimony Wyckoff symmetric positions. The experimental lattice parameters and B_0 of the elements are reproduced within 3% and 18%, respectively. For antimony, the present calculations correctly predict that the most stable structure at 0 K is the $R\bar{3}m$, as found experimentally at LT. The calculated lattice parameters of $Cu_5In_2Sb_2$ differ by less than 1.2% from the experimental ones. The compound $Cu_5In_2Sb_2$ is thermodynamically stable with respect to the elements, while we predict the $Cu_5Sb_2In_2$ anti-site structure to be unstable. In

dx.doi.org/10.1021/ic3011794 | *Inorg. Chem.* 2012, 51, 10787−10792

Scheme 1. Group−Subgroup Relations between the Fundamental Space Group for NiAs/Ni_2In, $P6_3/mmc$, and the Uniquely Determined Subgroup $Bb2_1m$

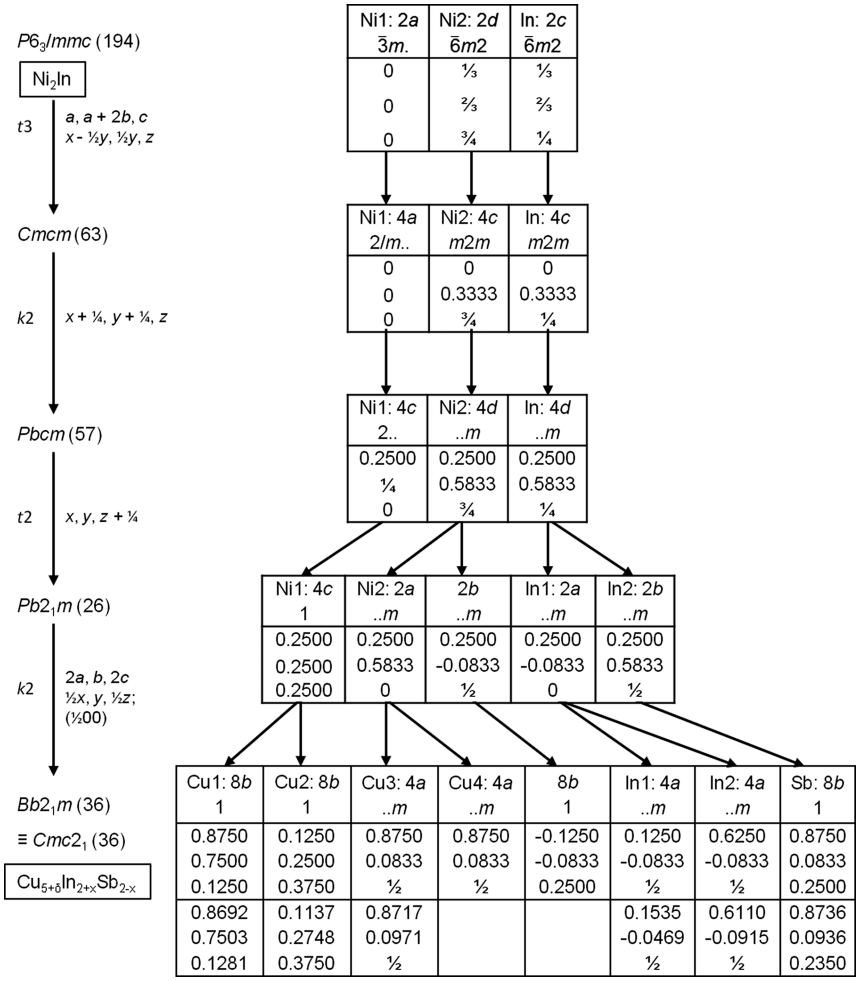

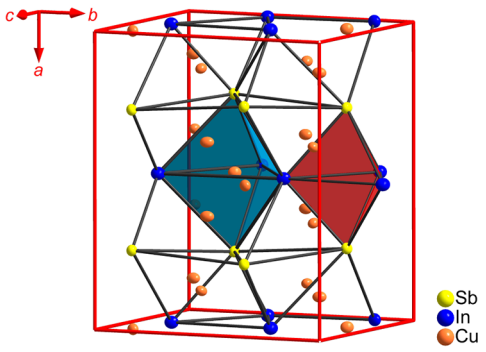

Figure 4. Idealized structure of $Cu_5In_2Sb_2$; thermal ellipsoid probability of 50%.

Table 3, the internal atomic positions for Sb, $Cu_5In_2Sb_2$, and $Cu_5In_2Sb_2$ are presented. The calculated positions are in very good agreement with those obtained in the experiment.

In Figure 5, the electronic density of states (DOS) calculated for the *ab initio* predicted equilibrium structures of $Cu_5In_2Sb_2$ and its anti-structure $Cu_5Sb_2In_2$ compound are depicted. Both $Cu_5In_2Sb_2$ and its anti-structure $Cu_5Sb_2In_2$ have metallic character with a relatively low value of the DOS at the Fermi level. The main contribution to the DOS comes from the d states of copper. The copper d band extends from −6 eV up to approximately the Fermi level. At lower energies, two bands can be distinguished. The first band, extending from −11.5 to −9.5 eV, is mainly determined by antimony states, whereas indium states dominate the second band, extending from −9.0 to −6.0 eV. Between the two bands, a pseudogap is located at about −9 eV. When the DOS of both compounds $Cu_5In_2Sb_2$ and $Cu_5Sb_2In_2$ are compared, it is found that there is a difference in the location of the second band. However, for the anti-structure $Cu_5Sb_2In_2$, the contribution of copper s states as well as indium and antimony s and p states is shifted to higher energies with respect to $Cu_5In_2Sb_2$. This shift causes a larger pseudogap, which extends from −9.5 to −8 eV, and could, in principle, explain the vast difference in the energies of formation of both compounds. For energies above the Fermi level, the electronic states of all species contribute to the determination of the shape of the DOS. Generally, the shapes of the DOS for both compounds are similar and follow the general trends that have been recently discussed for other structurally related binary Cu−In and Cu−Sn compounds.[32−34]

5. SUMMARY AND CONCLUDING REMARKS

A new ternary orthorhombic compound with the formula $Cu_{5.33}In_{2.29}Sb_{1.71}$ crystallizing in the space group $Cmc2_1$ and with 36 atoms per unit cell has been synthesized. Details of the experimental study and the structural parameters of this compound are reported in the first part of the work. In the

dx.doi.org/10.1021/ic3011794 | *Inorg. Chem.* 2012, 51, 10787−10792

Table 2. *Ab Initio* Calculated Structural and Elastic Properties for Cu, In, Sb, $Cu_5In_2Sb_2$, and $Cu_5Sb_2In_2$ at 0 K. For the intermetallic phases, the energy of formation from the elements in the given structures is reported.

			lattice parameters *a*, *c* (Å)				
element	space group	V_0 (Å^3/atom)	calculated	experimental	B_0 (GPa)	B_0'	ΔE_f (kJ/mol)
Cu-fcc	$Fm\bar{3}m$	12.035	3.638	3.596[a]	138.0, 142[b]	5.3, 5.5, 5.0[c]	
In-tI2	$I4/mmm$	27.512	3.305, 5.036	(3.245, 4.942)[d]	36.3, 41.8[e]	5.7, 4.81[e]	
Sb-hR2	$R\bar{3}m$	31.782	4.377, 11.491	(4.308, 11.274)[d]	31.5, 38.3[f]	8.8	
$Cu_5In_2Sb_2$	$Cmc2_1$	18.252, 17.758[g]	10.253, 8.576, 7.472	10.181, 8.456, 7.377[g]	81.3	6.2	−2.4867
$Cu_5Sb_2In_2$	$Cmc2_1$	18.394	10.446, 8.551, 7.414		79.0	6.5	2.2390

[a]Experimental data extrapolated to 0 K.[27] [b]Experimental data extrapolated to 0 K.[28] [c]Experimental data at 298 K.[29] [d]Experimental data at 291 K (In) and 298 K (Sb).[30] [e]Experimental data at 293 K.[31] [f]Experimental data.[32] [g]Experimental data from the present work.

Table 3. Sb, $Cu_5In_2Sb_2$, and $Cu_5Sb_2In_2$ Unit Cell Internal Coordinates Calculated Ab Initio, Compared with the Atomic Positions for the $Cu_5In_2Sb_2$ Intermetallic Compound Determined in the Present Work

		x, *y*, *z*	
	site	GGA	experiment
Sb	Sb: 6*c*	0.0, 0.0, 0.2333	0.0, 0.0, 0.23349
$Cu_5In_2Sb_2$	Cu1: 8*d*	0.1286, 0.6310, 0.2521	0.1282, 0.6308, 0.2515
	Cu2: 8*d*	0.3755, 0.6149, 0.2257	0.3750, 0.6137, 0.2271
	Cu3: 4*d*	0.5, 0.3714, 0.4046	0.5, 0.3717, 0.4044
	In1: 4*d*	0.5, 0.3465, 0.0478	0.5, 0.3465, 0.0480
	In2: 4*d*	0.5, 0.1078, 0.5935	0.5, 0.1113, 0.5923
	Sb1: 8*d*	0.2355, 0.3740, 0.4074	0.2352, 0.3736, 0.4072
$Cu_5Sb_2In_2$	Cu1: 8*d*	0.1284, 0.6306, 0.2542	
	Cu2: 8*d*	0.3744, 0.6152, 0.2251	
	Cu3: 4*d*	0.5, 0.3764, 0.4059	
	Sb1: 4*d*	0.5, 0.3466, 0.0518	
	Sb2: 4*d*	0.5, 0.1078, 0.5876	
	In1: 8*d*	0.2338, 0.3736, 0.4063	

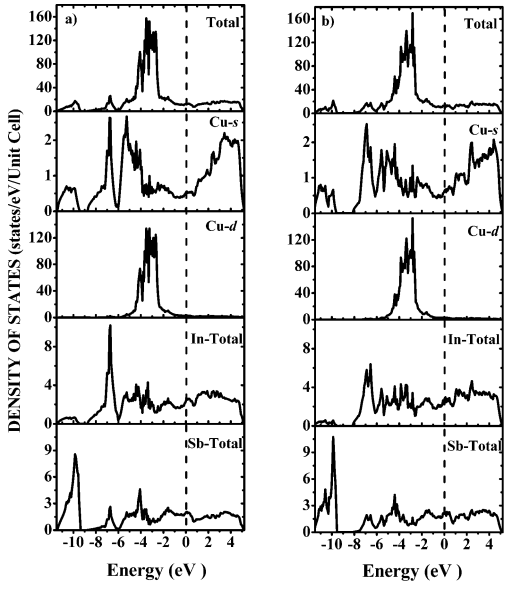

Figure 5. *Ab initio* calculated electronic DOS of (a) $Cu_5In_2Sb_2$ and (b) the anti-structure $Cu_5Sb_2In_2$ compound.

second part, *ab initio* calculations based on DFT and the PAW method are used to characterize the structural, thermodynamic, and electronic properties of (a) $Cu_5In_2Sb_2$ and (b) the anti-structure $Cu_5Sb_2In_2$ compound.

The present calculations include the lattice parameters, molar volume, bulk modulus and its pressure derivative, energy of formation from the elements, and the electronic DOS.

The calculated lattice parameters and internal atomic coordinates are in excellent agreement with the values determined experimentally. The $Cu_5In_2Sb_2$ compound is found to be thermodynamically stable with respect to the elements at 0 K.

These theoretical results for the $Cu_5In_2Sb_2$ phase have been compared with those for the $Cu_5Sb_2In_2$ anti-site structure compound, resulting from exchange of the In and Sb Wyckoff symmetric positions. The $Cu_5Sb_2In_2$ phase is thermodynamically unstable with respect to the elements at 0 K.

Both the $Cu_5In_2Sb_2$ and $Cu_5Sb_2In_2$ compounds show metallic behavior. The main contribution to the DOS comes from Cu d electrons, extending from −6 eV up to approximately the Fermi level.

■ ASSOCIATED CONTENT

Ⓢ Supporting Information

X-ray crystallographic data in CIF format. This material is available free of charge via the Internet at http://pubs.acs.org.

■ AUTHOR INFORMATION

Corresponding Author

*E-mail: carola.muller@polymat.lth.se.

Author Contributions

All authors have given approval to the final version of the manuscript.

Notes

The authors declare no competing financial interest.

■ ACKNOWLEDGMENTS

The authors are grateful to Gunnel Karlsson for supporting the EDXS measurements. This work was supported by the Swedish Research Council VR, the Agencia Nacional de Promoción Científica y Tecnológica (Grants BID 1728/OC-AR and PICT-2006 1947), and Universidad Nacional del Comahue (Project I157).

■ REFERENCES

(1) Subramanian, K. N., Ed. *Lead-Free Electronic Solders. A Special Issue of the Journal of Materials Science: Materials in Electronics*; Springer: Berlin, 2007.

(2) Liu, W. E.; Mohney, S. E. *Mater. Sci. Eng., B* **2003**, *103*, 189−201.

(3) Manasijevic, D.; Minic, D.; Zivkovic, D.; Vrestal, J.; Aljilji, A.; Talijan, N.; Stajic-Trosic, J.; Marijanovec, S.; Todorovic, R. *CALPHAD: Comput. Coupling Phase Diagrams Thermochem.* **2009**, *33*, 221−226.

(4) Okamoto, H. *J. Phase Equilib.* **1994**, *5*, 226−227.

(5) Bahari, Z.; Dichi, E.; Legendre, B.; Dugué, J. *Thermochim. Acta* **2003**, *401*, 131−138.
(6) Saunders, N.; Miodownik, A. P. *Bull. Alloy Phase Diagrams* **1990**, *11*, 278−287.
(7) Kattner, U. *JOM* **2002**, *54*, 45−51.
(8) Shim, J.-H.; Oh, Ch.-S.; Lee, B.-J.; Lee, D. N. *Z. Metallkd.* **1996**, *8*, 205−212.
(9) Massalski, T. B., Ed. *Binary Alloy Phase Diagrams*; 2nd ed.; ASM International: Metal Park, OH, 1996; pp 1424−1426.
(10) Elding-Pontén, M.; Stenberg, L.; Lidin, S. *J. Alloys Compd.* **1997**, *261*, 162−171.
(11) Lidin, S.; Larsson, A. K. *J. Solid State Chem.* **1995**, *118*, 313−322.
(12) Jandali, M. Z.; Rajasekharan, T. P.; Schubert, K. *Z. Metallkd.* **1982**, *73*, 463−467.
(13) Günzel, E.; Schubert, K. *Z. Metallkd.* **1958**, *49*, 124−133.
(14) Schubert, K.; Burkhardt, W.; Esslinger, P.; Günzel, E.; Meissner, H. G.; Schütt, W.; Wegst, J.; Wilkens, M. *Naturwissenschaften* **1956**, *43*, 248−249.
(15) Hofmann, W. *Z. Metallkd.* **1941**, *33*, 373.
(16) Nuss, J.; Jansen, M. *Z. Anorg. Allg. Chem.* **2002**, *628*, 1152−1157.
(17) Blöchl, P. E. *Phys. Rev. B: Condens. Matter Mater. Phys.* **1994**, *50*, 17953−17979.
(18) Kresse, G.; Furthmüller, J. *Comput. Mater. Sci.* **1996**, *6*, 15−50.
(19) *WinXPow, Powder Diffraction Software*, version 3.1; Stoe & Cie: Darmstadt, Germany, 2011.
(20) *CrysAlisPro*, version 1.171.35.6; Oxford Diffraction Ltd.: Abington, U.K.,2011.
(21) Oszlanyi, G.; Suto, A. *Acta Crystallogr., Sect. A: Found. Crystallogr.* **2004**, *60*, 134−141.
(22) Oszlanyi, G.; Suto, A. *Acta Crystallogr., Sect. A: Found. Crystallogr.* **2005**, *61*, 147−152.
(23) Palatinus, L.; Chapuis, G. *J. Appl. Crystallogr.* **2007**, *40*, 786−790.
(24) Petricek, V.; Dusek, M.; Palatinus, L. *Jana2006. The crystallographic computing system*; Institute of Physics: Praha, Czech Republic, 2006.
(25) *Aztec*, version 1.0; Oxford Instruments Nanotechnology, Tools Ltd.: Oxford, U.K., 2010−2011.
(26) Perdew, J. P.; Wang, Y. *Phys. Rev. B: Condens. Matter* **1991**, *44*, 13298−13307.
(27) Straumanis, M. E.; Yu, L. S. *Acta Crystallogr., Sect. A: Cryst. Phys., Diffr., Theor. Gen. Crystallogr.* **1969**, *25*, 676−682.
(28) Overton, W. C., Jr.; Gaffney, J. *Phys. Rev.* **1955**, *98*, 969−977.
(29) Steinberg, D. J. *J. Phys. Chem. Solids* **1982**, *43*, 1173−1175.
(30) Villars, P. *Pearson's Handbook Desk Edition*; ASM International: Materials Park, OH, 1997.
(31) Takemura, K. *Phys. Rev. B: Condens. Matter Mater. Phys.* **1991**, *44*, 545−549.
(32) Kittel, C. *Introduction to solid state physics*; 7th ed.; Wiley: New York, 1996.
(33) Ramos de Debiaggi, S.; Cabeza, G. F.; Deluque Toro, C.; Monti, A. M.; Sommadossi, S.; Fernández Guillermet, A. *J. Alloys Compd.* **2011**, *509*, 3238−3245.
(34) Ramos de Debiaggi, S.; Deluque Toro, C.; Cabeza, G. F.; Fernández Guillermet, A. *J. Alloys Compd.* **2012**, http:dx.doi.org/10.1016/j.jallcom.2012.06.138.